

Coexistence of Localized and Delocalized Surface Plasmon Modes in Percolating Metal Films

K. Seal,¹ D. A. Genov,² A. K. Sarychev,³ H. Noh,¹ V. M. Shalaev,⁴ Z. C. Ying,⁵ X. Zhang,² and H. Cao¹

¹*Department of Physics and Astronomy, Northwestern University, Evanston, Illinois 60208, USA*

²*NSF Nanoscale Science and Engineering Center, University of California–Berkeley, Berkeley, California 94720, USA*

³*Ethertronics, Inc., 9605 Scranton Road, Suite 850, San Diego, California 92121, USA*

⁴*School of Electrical and Computer Engineering, Purdue University, West Lafayette, Indiana 47907, USA*

⁵*Division of Materials Research, National Science Foundation, Arlington, Virginia 22230, USA*

(Received 30 March 2006; published 17 November 2006)

Near-field intensity statistics in semicontinuous silver films over a wide range of surface coverage are investigated using near-field scanning optical microscopy. The variance of intensity fluctuations and the high-order moments of intensity enhancement exhibit local minima at the percolation threshold. This reduction in local field fluctuations results from resonant excitation of delocalized surface plasmon modes. By probing the modification of the critical indices for high-order moments of intensity enhancement caused by the delocalized states, we provide the first experimental evidence for the coexistence of localized and delocalized surface plasmon modes in percolating metal films.

DOI: [10.1103/PhysRevLett.97.206103](https://doi.org/10.1103/PhysRevLett.97.206103)

PACS numbers: 68.37.Uv, 42.25.Dd, 73.20.Mf, 78.67.–n

Studies of field and intensity statistics have deepened our understanding of mesoscopic transport and localization in disordered systems [1]. In dielectric random media, the variance of intensity fluctuations reflects the extent of photon localization, even in the presence of absorption [2]. In disordered metallic nanostructures, however, the intensity statistics are more complex because of strong interactions between light and intrinsic material excitations—surface plasmons (SPs) [3,4]. Such interactions can lead to spatial localization of electromagnetic energy at subwavelength scales and giant local field fluctuations [5–9]. Near-field intensity statistics have been obtained numerically [7–11] and experimentally [12,13] to characterize the local field fluctuations in various metal aggregates, fractal structures, rough and semicontinuous metal films. The probability density function of intensity enhancement in the multiple scattering regime is shown to be distinctly different from that in the single scattering regime [12]. However, the exact relation between the intensity statistics and SP localization remains unclear.

In the early theoretical studies on random metal-dielectric composites [14], the similarity between the Kirchhoff Hamiltonian used to describe the system and the Anderson Hamiltonian led to the expectation that all surface plasmon eigenmodes were localized [14]. Follow-up computer simulations illustrated that a planar disordered nanosystem can simultaneously have localized and delocalized states [15]. This concept of inhomogeneous localization was originally introduced for metal fractal aggregates, where self-similarity in the structural geometry can result in a mode consisting of multiple hot spots spread over the entire system [8]. The latest calculations reveal that in an infinitely large semicontinuous metal film, delocalized SP modes exist only at one point in the eigenvalue spectrum and their measure is zero [16]. The physical origin for the delocalized states lies in the short-range

correlations in the governing Kirchhoff Hamiltonian, which are absent in the Anderson Hamiltonian. Even though they have a zero measure, delocalized modes affect the local field statistics by modifying the critical indices for the high-order field moments. Despite these theoretical predictions, inhomogeneous localization of SP modes has not been confirmed experimentally.

This Letter provides the first experimental evidence for the coexistence of localized and delocalized SP modes in semicontinuous metal films at the percolation threshold. Using near-field scanning optical microscopy (NSOM), we investigated the near-field intensity statistics on the surface of semicontinuous silver films over a wide range of surface coverage of silver p . Near the percolation threshold, the variance of intensity fluctuations and the high-order moments of intensity enhancement exhibit local minima, indicating a reduction in the local field fluctuations. By comparing the measured scaling exponents of high-order moments to the numerically calculated values, we extract the degree of delocalization through an estimation of the effective delocalization index γ at the percolation threshold.

Semicontinuous silver films on glass substrates were synthesized by pulsed laser deposition [13]. Transmission electron microscope (TEM) images show that the samples are composed of silver grains with an average size of 10–15 nm. An increase in deposition time (surface concentration of silver p) induces a structural transition from isolated silver grains ($p \leq 0.4$) to interconnected metal clusters ($p \approx 0.6$) and finally to a nearly continuous metal film with dielectric voids ($p \geq 0.8$). For these samples, the percolation threshold was found to be at $p_c \approx 0.65$ [13]. In the near-field experiment, the samples were illuminated by the evanescent field (in total internal reflection geometry) of He-Ne lasers operating at 543 and 633 nm (p polarized). The local optical signal was collected by a tapered, un-

coated optical fiber with a tip radius ~ 50 nm. The tip-to-sample distance, controlled by shear-force feedback, was about 10 nm. The spatial resolution was estimated to be approximately 150 nm from the smallest features present in the near-field images [13]. Hot spots of various sizes and intensities were clearly seen in the near-field images [17]. Fourier analysis of the spatial intensity distribution revealed that the scattering strength is maximum at p_c .

From the NSOM images, the variance of intensity fluctuations $\text{var}(I) = \langle I(x, y)^2 \rangle / \langle I(x, y) \rangle^2 - 1$ was computed for semicontinuous silver films of different p . Figure 1 shows the experimental data of $\text{var}(I)$ as a function of $\Delta p = p - p_c$ at a probe wavelength of 633 nm. Each data point was obtained from approximately 300 000 near-field intensity values. The error bar was evaluated as the standard error of data collected from several NSOM images of different parts of the samples. Unexpectedly, the intensity fluctuations do not maximize at p_c ($\Delta p = 0$), where scattering is the strongest. Instead, a local minimum appears at p_c . Away from p_c , $\text{var}(I)$ has two maxima at $\Delta p \approx -0.2$ and $\Delta p \approx +0.1$. A similar dependence of $\text{var}(I)$ on p was observed at the other probe wavelength 543 nm. However, the absolute value of $\text{var}(I)$ at $\lambda = 543$ nm is lower than that at $\lambda = 633$ nm, indicating that the intensity fluctuations are stronger at longer wavelengths.

The variance of intensity fluctuations is proportional to the inverse participation ratio of the local field R_{IP} , often used to describe the spatial extent of eigenstates [10,11]. In the current experiment where the incident field excites a number of SP modes, R_{IP} gives a qualitative measure of the surface area occupied by hot spots. Similar to $\text{var}(I)$, R_{IP} has a minimum at p_c and two maxima on either side. Larger values of R_{IP} at $|p - p_c| \approx 0.1$ and 0.2 indicate that a smaller percentage of the film surface is occupied by hot spots. This is consistent with the direct observation that away from p_c there are fewer hot spots but each is brighter. The experimentally observed dip in R_{IP} suggests a weakening of SP localization strength at p_c .

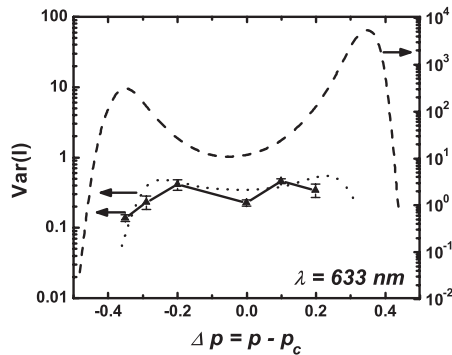


FIG. 1. Near-field intensity variance $\text{var}(I)$ as a function of silver concentration $\Delta p = p - p_c$, obtained experimentally (solid line with triangles) and numerically with (dotted line) and without (dashed line) spatial averaging.

From the near-field images, the high-order moments of intensity enhancement $M_{2n} = \langle I(x, y)^n \rangle / I_0^n$ were computed, where the incident light intensity I_0 was obtained from the near-field measurement of a clean glass substrate. Figure 2(a) is a plot of M_{2n} vs Δp for $n = 2, 3, 4$, and 5. The error bars were obtained by the same method as for $\text{var}(I)$ in Fig. 1. M_{2n} exhibits a prominent dip near p_c , which becomes more pronounced for higher n . This observation indicates once more that the local field fluctuations are weakened at the percolation threshold.

Numerical simulations were performed to interpret the above experimental findings. In the visible frequency regime, metal-dielectric composites can be viewed as a system of lumped RLC circuits [7], and the bond percolation model can be employed to describe their electromagnetic response. Detailed information on our method of calculation is presented in Refs. [11,16]. The bond model has a percolation threshold $p_c = 0.5$, which differs slightly from experiment. This deviation, however, should not preclude a direct mapping between experiment and theory because the scaling properties of random metal films do not depend on the absolute value of p_c [18]. In the numerical simulations, the local field distribution was calculated for $2 \mu\text{m} \times 2 \mu\text{m}$ semicontinuous films of different silver concentrations. At the percolation threshold a highly inhomogeneous local field distribution is observed, with peak intensities surpassing the incident laser light intensity by factors of 10^3 – 10^4 . The experimentally obtained local field enhancements are considerably lower because of the finite spatial resolution of NSOM. For comparison with the experimental data, the local fields at a distance equal to the tip-sample separation (~ 10 nm) from the sample surface were estimated and then averaged with the NSOM aperture function (corresponding to a tip resolution of ~ 150 nm). Both $\text{var}(I)$ and M_{2n} were then obtained from up to 1000 realizations of the random metal-dielectric system at a fixed p . Numerical data obtained before and after the spatial averaging are presented in Figs. 1 and 2.

As shown in Fig. 1, $\text{var}(I)$ calculated without spatial averaging exhibits a wider and deeper dip near p_c . The spatial averaging not only reduces the value of $\text{var}(I)$ but also partially smooths out the dip at p_c . After the resolution limit of our NSOM is taken into account, the numerical data closely follow the experimental $\text{var}(I)$. However, some of the numerical values fall outside the experimental error bars because of inevitable approximations used in the calculations. For example, there is some uncertainty in the value of dielectric constant of silver ϵ_m , the tip-sample distance and the spatial averaging parameter are not exact. Nevertheless, the difference between the measured and calculated values of $\text{var}(I)$ is small. In Fig. 2, the calculated local field moments M_{2n} exhibit a p dependence similar to the measured one, viz., M_{2n} reaches a local minimum at p_c and has two distinct maxima at $|\Delta p| \lesssim 0.3$. The above numerical uncertainties also contribute to the discrepancies

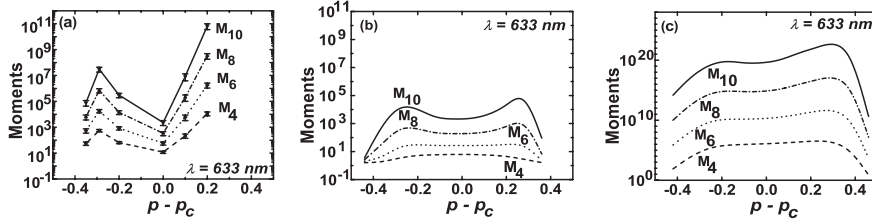


FIG. 2. High-order moments of near-field intensity enhancement M_{2n} as a function of silver concentration $\Delta p = p - p_c$, obtained experimentally (a) and numerically with (b) and without (c) spatial averaging.

between experimental and numerical (spatially averaged) data in Fig. 2.

The observed decrease of $\text{var}(I)$ and M_{2n} at $|\Delta p| \geq 0.3$ can be explained by the resonant nature of SP excitation. According to percolation theory [7,18,19], the largest metal cluster in a random composite has a size $l_m(p) = ap_c^\nu/|p - p_c|^\nu$, where a is the average metal particle size, and ν is a critical exponent. Resonant SP modes can be excited by incident light of a wavelength λ if $l_m(p) \geq l_r = a(|\epsilon'_m|/\epsilon_d)^{\nu/(s+t)}$, where $\epsilon_m = \epsilon'_m + i\epsilon''_m$ and ϵ_d are the dielectric constants of the metal particles and dielectric host, respectively [7]. The critical exponents s and t correspond to the scaling of the composite's static conductivity and dielectric constant, respectively, with the sample size. For the planar systems under consideration, $s = \nu = t = \frac{4}{3}$ [18]. Thus the SP resonance wavelength in a cluster of size $l \geq l_r$ scales with l/a as $\lambda_r \approx \lambda_p(l/a)^{\nu/(s+t)} \approx \lambda_p\sqrt{l/a}$, where λ_p is the plasma wavelength [7]. This remarkable property of localized SPs is distinct from resonances in the retarded (nonquasistatic) regime.

When the metal concentration p differs considerably from p_c , there is a decrease in the maximum cluster size l_m . If $l_m(p) < l_r$, SP modes in the semicontinuous metal film can no longer be excited by the external field, leading to a dramatic decrease in the local electromagnetic response. The cutoff metal concentrations are estimated from the condition $l_r = l_m(p_\pm)$ as $p_\pm = p_c[1 \pm (\epsilon_d/|\epsilon'_m|)^{1/(s+t)}]$. At $\lambda = 633$ nm, $\Delta p_\pm = |p_\pm - p_c| \approx 0.3$. For concentrations in the range $|\Delta p| > \Delta p_\pm$, both $\text{var}(I)$ and M_{2n} are expected to decrease sharply. Estimates for the cutoff concentrations Δp_\pm agree well with the experimental and numerical results shown in Figs. 1 and 2. The presence of cutoff metal concentrations also manifests itself as an anomalous absorption band in semicontinuous metal films [20]. Specifically, when $\kappa = |\epsilon''_m/\epsilon'_m| \ll 1$, the buildup of giant local fields and storage of electromagnetic energy in the films lead to strong light absorption, which occurs for metal concentrations inside the band $p_c - \Delta p_- < p < p_c + \Delta p_+$ [21]. The quantity Δp_\pm , calculated as $\sqrt{|\epsilon'_m|\epsilon_d/(|\epsilon'_m| + \epsilon_d)}$ from effective medium theory, gives values close to the cutoff concentration estimates based on the resonant cluster size.

The minima in $\text{var}(I)$ and M_{2n} at p_c can be understood by solving the SP eigenproblem $\nabla \cdot [\epsilon(\mathbf{r})\nabla\Psi_\Lambda(\mathbf{r})] = \Lambda\Psi_\Lambda(\mathbf{r})$, where Λ is the eigenvalue, Ψ_Λ is the eigenstate, and $\epsilon(\mathbf{r})$ is the local permittivity that takes values ϵ_m and

ϵ_d in metal and dielectric regions of the film correspondingly [14]. As detailed in Refs. [7,11], a spatial renormalization procedure is applied for frequencies below the single particle resonance. Cross correlations between the diagonal and off-diagonal elements of the Kirchhoff Hamiltonian originate from charge current conservation and lead to delocalization of the SP eigenmodes [11]. Under excitation by a uniform external field, the high-order moments M_{2n} can be estimated as an expansion of the local potential over the eigenspace:

$$M_{2n} \simeq \left(\frac{|\epsilon'_m|}{\epsilon_d}\right)^{(2\nu(n-1)+s/s+t)} \int_{-\infty}^{\infty} \frac{\rho(\Lambda)[a/\xi(\Lambda)]^{2(2n-1)}}{(\Lambda^2 + \kappa^2)^n} d\Lambda \\ \simeq \left(\frac{|\epsilon'_m|}{\epsilon_d}\right)^{n-(1/2)} \kappa^{-\kappa_{2n}}, \quad (1)$$

where ρ is the density of SP eigenstates, ξ is the localization length, and $\kappa_{2n} = (2n-1)(1-2\gamma) + \gamma$ is a scaling exponent. In the limit $\Lambda \rightarrow 0$, both ρ and ξ diverge as $|\Lambda|^{-\gamma}$. The SP delocalization index has been previously estimated as $\gamma = 0.14$ at p_c [16]. Because κ has a small but nonzero value, all states with $|\Lambda| \leq \kappa$ are resonantly excited. For a large system, only a small fraction of the excited states are fully delocalized, i.e., their localization length $\xi(\Lambda)$ exceeds the system size L . Nevertheless, the resonant excitation of these states at p_c reduces the value of field moments as compared to that at $\gamma = 0$ (where all states are localized), i.e., $M_{2n}(\gamma = 0.14) < M_{2n}(\gamma = 0)$. As p deviates from p_c , our numerical calculations show a notable decrease in the localization length ξ of excited SP eigenstates. This decrease may be understood intuitively to be caused by a reduction in the maximum size of the resonating metal clusters with increase in $|p - p_c|$.

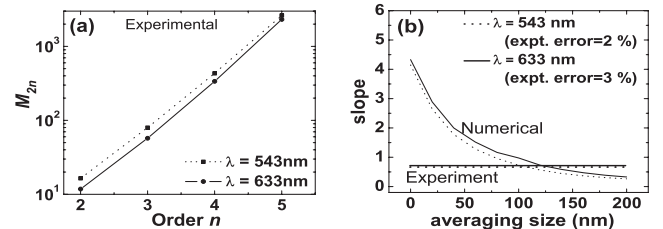


FIG. 3. (a) Log-linear plot of measured high-order moments of near-field intensity enhancement M_{2n} vs n . (b) Slope of $\log(M_{2n})$ over n obtained numerically after spatial averaging versus averaging parameter d . The measured slopes are marked by horizontal lines with the standard error given in the legend.

Stronger localization leads to larger local field fluctuations, which explains the increase of variance and field moments away from p_c . Therefore, the double-peaks in $\text{var}(I)$ and M_{2n} result from the interplay of two factors: as $|\Delta p|$ increases the resonantly excited SP modes become more localized, meanwhile their number decreases, especially beyond Δp_{\pm} .

To experimentally confirm the coexistence of localized and delocalized states in the percolating silver film, we probe the scaling exponent κ_{2n} of the high-order intensity moments M_{2n} . The singularity of ξ and ρ at $\Lambda = 0$ modifies κ_{2n} by introducing a nonzero delocalization index γ [16]. Figure 3(a) is a log-linear plot of the measured M_{2n} versus order n at p_c for two probe wavelengths 543 nm and 633 nm. $\log(M_{2n})$ increases linearly with n . Scaling theory, as seen in Eq. (1), also predicts a linear dependence with a slope $2(2\gamma - 1)\log(\kappa) + \log(|\epsilon'_m|/\epsilon_d)$. However, because of the limited NSOM resolution, the slopes obtained experimentally are considerably lower than those obtained numerically. To account for the effect of finite spatial resolution, the calculated local field distribution was first averaged over an area of dimension d , then M_{2n} was computed to extract the slope of $\log(M_{2n})$ vs n . Figure 3(b) shows that the slopes decrease as d increases. When the slopes are reduced to the experimental values (marked by horizontal lines), the averaging parameter d is very close to our NSOM resolution estimated from the smallest features in the near-field images. The same value of d also leads to good agreement between the calculated $\text{var}(I)$ and the experimental data. This corroboration provides experimental validation of our numerical results with the delocalization index $\gamma \approx 0.1$. Hence, our experimental measurement confirms a tangible presence of delocalized SP modes at p_c .

Finally, we point out that when p is sufficiently away from p_c , semicontinuous silver films support propagating surface waves via collective excitations [17]. For example, at high silver coverage, impinging light excites surface plasmon polaritons (SPPs) which propagate across the film. These SPPs experience scattering and interference which lead to intensity modulations [17]. Because of this, the measured high-order moments M_{2n} are larger than the numerical values obtained from the quasistatic calculation at p away from p_c in Fig. 2. Near p_c , substantial structural inhomogeneities cause strong scattering and suppress propagating surface waves. As a result, the incident light couples predominately to SP modes, and the near-field intensity statistics are dominated by the excited SP modes. This conclusion is confirmed by the good agreement between the experimental and numerical data of M_{2n} at p_c in Fig. 2.

In summary, we have studied the near-field intensity statistics in semicontinuous silver films over a wide range of metal concentrations. The variance of intensity fluctuations and the high-order moments of intensity enhancement exhibit local minima at the percolation threshold. The

reduction in local field fluctuations results from resonant excitation of delocalized SP modes. Despite their zero measure, the delocalized states modify the critical exponents of the high-order moments of intensity enhancement. By comparing experimental data with numerical results, we obtain the effective delocalization index at the percolation threshold. This work provides the first experimental evidence for the existence of delocalized SP modes in the strong scattering regime, and thus confirms the coexistence of localized and delocalized SP modes in metallic random systems.

This work is funded by NSF Grant No. DMR-0093949, NSF-MRSEC Grant No. DMR-00706097, ARO Grant No. DAAD19-01-1-0682, SINAM and NSF-NSEC Grant No. DMI-0327077, and NSF-NIRT Grant No. ECS-0210445.

-
- [1] *The Scattering and Localization of Classical Waves*, edited by P. Sheng (World Scientific, Singapore, 1990).
 - [2] A. A. Chabanov, M. Stoytchev, and A. Z. Genack, *Nature (London)* **404**, 850 (2000).
 - [3] V. M. Shalaev, *Nonlinear Optics of Random Media* (Springer, Berlin, 2000).
 - [4] *Optics of Nanostructured Materials*, edited by V. M. Markel and T. F. George (Wiley, New York, 2001).
 - [5] D. P. Tsai *et al.*, *Phys. Rev. Lett.* **72**, 4149 (1994); S. Gresillon *et al.*, *Phys. Rev. Lett.* **82**, 4520 (1999); S. Ducourtieux *et al.*, *Phys. Rev. B* **64**, 165403 (2001).
 - [6] S. I. Bozhevolnyi, I. I. Smolyaninov, and A. V. Zayats, *Phys. Rev. B* **51**, 17916 (1995); S. I. Bozhevolnyi, V. S. Volkov, and K. Leosson, *Phys. Rev. Lett.* **89**, 186801 (2002).
 - [7] A. K. Sarychev and V. M. Shalaev, *Phys. Rep.* **335**, 275 (2000).
 - [8] M. I. Stockman, in *Optics of Nanostructured Materials* (Ref. [4]), p. 313.
 - [9] J. A. Sánchez-Gil, J. V. García-Ramos, and E. Méndez, *Phys. Rev. B* **62**, 10515 (2000).
 - [10] L. Zekri *et al.*, *J. Phys. Condens. Matter* **12**, 283 (2000).
 - [11] D. A. Genov, A. K. Sarychev, and V. M. Shalaev, *Phys. Rev. E* **67**, 056611 (2003).
 - [12] S. I. Bozhevolnyi and V. Coello, *Phys. Rev. B* **64**, 115414 (2001).
 - [13] K. Seal *et al.*, *Phys. Rev. B* **67**, 035318 (2003).
 - [14] A. K. Sarychev, V. A. Shubin, and V. M. Shalaev, *Phys. Rev. B* **60**, 16389 (1999).
 - [15] M. I. Stockman, S. V. Faleev, and D. J. Bergman, *Phys. Rev. Lett.* **87**, 167401 (2001).
 - [16] D. A. Genov, A. K. Sarychev, and V. M. Shalaev, *Phys. Rev. B* **72**, 113102 (2005).
 - [17] K. Seal *et al.*, *Phys. Rev. Lett.* **94**, 226101 (2005).
 - [18] D. Stauffer and A. Aharony, *Introduction to Percolation Theory* (Taylor and Francis, London, 1992), 2nd ed.
 - [19] Y. Yagil *et al.*, *Phys. Rev. B* **46**, 2503 (1992).
 - [20] P. Gadenne, A. Beghadi, and J. Lafait, *Opt. Commun.* **65**, 17 (1988).
 - [21] F. Brouers *et al.*, *Phys. Rev. B* **47**, 666 (1993).